PHYSICAL REVIEW B VOLUME 47, NUMBER 19 15 MAY 1993-I

Effects of interchain interactions on the electronic structure of heavily doped *trans*-polyacetylene

S. Stafström
Department of Physics, Linköping University, S-581 83 Linköping, Sweden
(Received 14 October 1992)

The effects of interchain interactions on the geometrical and electronic structure of heavily doped *trans*-polyacetylene are studied in detail. The interchain interactions include electron hopping, electron-electron repulsion, and the potential due to counterions associated with neighboring chains. The optimized geometry corresponds to that of a soliton lattice for dopant concentration up to 12.5%, which is the highest concentration included in this study. The interchain interactions reduce the energy gap around the Fermi energy considerably. A sharp transition into a metallic state is observed at dopant concentrations around 9%. The metallic state is understood from the fact that the optimized dimerization amplitude is small in the case of a strongly interacting soliton lattice. In this situation, the Peierls gap is of the same magnitude as the broadening of the energy bands due to interchain interactions. The effects of disorder on the electronic structure are also discussed. Three-dimensional delocalization of the electronic states is observed for realistic values of the interchain-hopping strength.

I. INTRODUCTION

The quasi-one-dimensional nature of conjugated polymers gives rise to many of the fundamental properties of these materials. A general feature of one-dimensional systems is the strong coupling between the electronic system and the lattice (the phonons). This coupling is clearly manifested in the case of *trans*-polyacetylene [*trans*-$(CH)_x$] where the Peierls effect creates a gap around the Fermi energy and a corresponding dimerization of the lattice. The strong electron-phonon coupling also effects the fundamental excitation properties of conjugated polymers, which include the formation of localized quasiparticles such as solitons, polarons, and bipolarons.

It is well known that doping of π-conjugated polymers results in a highly conducting state of the polymer. However, the quasi-one-dimensional character of the polymers causes the effects of the doping to differ considerably from those observed in conventional three-dimensional inorganic semiconductors. The strong electron-phonon coupling leads to the formation of solitons or bipolarons upon charge transfer from the dopant species to the polymer.[1,2]

In addition to the strong intrachain interactions, there are also interactions between the polymer chains. These interactions, however weak at each individual carbon site, add up along the chains and give rise to a specific interchain ordering of the bond-length alternation pattern along the chains.[3] The interchain interactions are also important since they allow for charge transport between the chains, an effect which is of fundamental importance for the macroscopic conductivity present in doped conjugated polymers. Since very high conductivities can be obtained in doped *trans*-$(CH)_x$,[4,5] it is clear that the interchain interactions cannot be small.

The interchain interactions also affect the static electronic properties of polymeric materials. As discussed above, strictly one-dimensional solids always exhibit a finite gap around the Fermi energy and are therefore nonmetallic. A number of experimental data exist, however, which show that heavily doped conjugated polymers indeed have metallic properties. The transition into a metallic state for doped *trans*-$(CH)_x$ is observed as a sharp increase in the Pauli susceptibility at a critical dopant concentration around $y=0.06$.[6,7] Measurements of the optical conductivity of heavily doped *trans*-$(CH)_x$ show electronic transitions in the infrared region of the spectrum which are typical for a metal.[8] The importance of the interchain interactions as concerns the metallic properties of the doped polymers are clearly manifested in results on doped polymers in solution for which no metallic properties are observed even at very high dopant concentrations.[9]

The effects of interchain interactions on doping-induced defects such as solitons, polarons, and bipolarons have recently attracted some interest. Vogel and Campbell[10] have argued that these type of interactions can lead to a destabilization of the polaron in favor of ridged band states. This effect has also been discussed by Baeriswyl and Maki.[11] Wolf and Fesser[12] have treated the effects of disorder in the interchain hopping. Their studies show a decreasing dimerization and a corresponding enhancement of the density of states in the gap as a function of increasing disorder in the interchain coupling. The effect of interchain interactions on the metallic properties of doped *trans*-$(CH)_x$ was studied by Stafström[13] in a simplified version of the model presented here. These studies pointed out the importance of performing geometry optimization in order to take full account of the interchain interactions. Mizes and Conwell[14] have studied the effects of interchain coupling on the electronic structure of alkali-doped *trans*-$(CH)_x$. They conclude that interchain interactions alone are not the mechanism for the transition into a metallic state. The results presented in this paper do not support these results. Here, we have extended the investigation of the factors that are important for the transition into a low-band-gap system. Special emphasis is put on the role played by the

counterions as concerns the interchain interactions. It has been shown by Cohen and Glick[15] that intercalated charged species enhance the interchain hopping. This leads to an increase in the interchain interactions with increasing dopant concentration, a phenomenon which agrees with the observed increase in the macroscopic conductivity over the full regime of dopant concentrations.[4,5]

In this paper we use a Pariser-Parr-Pople-type of Hamiltonian to calculate the electronic structure of heavily doped *trans*-$(CH)_x$. The calculations that are performed at different dopant concentrations on systems of interacting chains include full geometry optimizations of the bond-length dimerization of the polymers. The Hamiltonian used in the calculations and the geometry optimization procedure are described in Sec. II. Section III contains the results, which are presented as follows: III A and III B deal with the lattice configuration and the energy gap of perfectly ordered systems, respectively. The effects of disorder are discussed briefly in III C and III D, finally, contains a discussion about interchain delocalization. A summary of the results is given in Sec. IV.

II. METHODOLOGY

The Hamiltonian considered for the studies of interacting *trans*-$(CH)_x$ chains is expressed in terms of a summation of Hamiltonians associated with a single chain $H^{(j)}$ over the number of chains contained in the system.

$$H=\sum_{j=1}^{3} H^{(j)} . \tag{1}$$

In this case we consider sodium-doped *trans*-$(CH)_x$. The crystal structure for this compound at the dopant concentration where the system becomes metallic is depicted in Fig. 1.[16] As a model system to this polymer crystal, we consider the interaction between the three chains surrounding a single column of sodium dopants. This approximation is based on the observation that interactions between such clusters of polymer chains are rather weak.[17] The sum of Eq. (1) thus contains three terms, $H^{(1)}$, $H^{(2)}$, and $H^{(3)}$, one for each chain in the system. Each of these Hamiltonians contains the following terms:

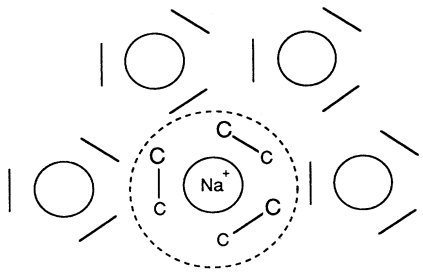

FIG. 1. Three-dimensional structure of sodium-doped *trans*-$(CH)_x$. The structure is viewed perpendicular to the direction of the polymer chains. The encircled part corresponds to the system of three chains treated in this work.

$$H^{(j)}=H^{(j)}_{\mathrm{SSH}}+H^{(j)}_{C}+H^{(j)}_{\mathrm{el\text{-}el}}+H^{(j)}_{\perp} . \tag{2}$$

H_{SSH} is the Su-Schrieffer-Heeger Hamiltonian[1] describing the electron-phonon interaction and the elastic energy of the lattice

$$H^{(j)}_{\mathrm{SSH}}=-\sum_{i,\sigma}(t_0-\alpha y_{j,i,i+1})(c^{\dagger}_{j,i+1,\sigma}c_{j,i,\sigma}+c^{\dagger}_{j,i,\sigma}c_{j,i+1,\sigma}) + \frac{K}{2}\sum_{i} y^2_{j,i,i+1} , \tag{3}$$

where $y_{j,i,i+1}$ describes the deviation from uniform bond lengths between sites i and $i+1$ of chain j, α is the electron-phonon coupling constant ($\alpha=4.1$ eV/Å), t_0 is the hopping between neighboring carbon sites in the case of uniform bond lengths ($t_0=2.5$ eV), and K is the effective spring constant which depends on the strength of the σ bond in the classical approximation ($K=21.0$ eV/Å^2).

H_C describes the interaction between the π electrons and the dopant ions. This term includes the effect from all dopants in the channel, i.e., also those associated with the two other chains in the three chain system (see Fig. 1).

$$H^{(j)}_{C}=\sum_{i,\sigma} V^{\mathrm{imp}}_{i} c^{\dagger}_{j,i,\sigma}c_{j,i,\sigma} . \tag{4}$$

V^{imp}_i is the electrostatic potential at site i due to all dopant ions in the system. An exponentially screened version of the Coulomb expression is used to represent this potential:

$$V^{\mathrm{imp}}_{i}=-e^2\sum_{n}\frac{1-\eta_{i,i_n}[1-\exp(-\gamma r_{i,i_n})]}{\varepsilon_1[r^2_{i,i_n}+d^2]^{1/2}} . \tag{5}$$

The exponential screening in Eq. (4) is controlled by the two parameters γ and η_{i,i_n}. It has been shown that the dopant-ion potential, within the first few bond lengths away from the dopant ion, shows a typical $1/r$ dependence, whereas for larger separations, the potential becomes exponentially screened.[18] This situation has been simulated by introducing the factor η_{i,i_n} which is defined as $\eta_{i,i_n}=\min(|i-i_n|/4,1)$, where i_n is the site opposite to a dopant ion. For separation larger than three bonds, the exponential screening is fully developed, whereas the sites opposite to the counterion experiences a pure $1/r$ potential. The value of γ(0.372 Å) is chosen in such a way that the potential produced by Eq. (4) is fitted to that calculated by Conwell, Mizes, and Jeyadev.[18]

$H_{\mathrm{el\text{-}el}}$ in Eq. (2) expresses the electron-electron interaction

$$H^{(j)}_{\mathrm{el\text{-}el}}=\tfrac{1}{2}\sum_{i,i',\sigma,\sigma',j'} U_{i,i'}c^{\dagger}_{j,i,\sigma}c_{j,i,\sigma}c^{\dagger}_{j',i',\sigma'}c_{j',i',\sigma'} . \tag{6}$$

In this case, these interactions are treated within the self-consistent field, Hartree-Fock approximation, which gives the following mean-field, spin-polarized electron-electron interaction Hamiltonian:

$$H^{(j)}_{\text{el-el}}=\tfrac{1}{2}\sum_{i,i'}\sum_{\sigma,\sigma'}\sum_{j'=1}^{3}U_{i,i'}(P^{\sigma'}_{j',i',i'}c^{\dagger}_{j,i,\sigma}c_{j,i,\sigma}-P^{\sigma'}_{j',i',i'}c^{\dagger}_{j,i,\sigma}c_{j,i,\sigma}\delta_{i,i}\delta_{\sigma,\sigma'}\delta_{j,j'}) \ . \tag{7}$$

Here, $P_{j,i,i}$ is the charge density at site i of the jth chain and $U_{i,i'}$ is the effective Coulomb integral between $2p_z$ orbitals attached to sites i and i' on the jth and j'th polymer chain, respectively. Note that this expression takes into account both intrachain and interchain electron-electron repulsions. The screened Ohno formula is adopted for the Coulomb integrals:[19]

$$U_{i,i'}=\frac{U_0 e^{-\gamma|r_{ii'}|}}{(1+0.6117r^2_{ii'})^{1/2}} \ , \tag{8}$$

where $U_0=5.56$ eV and $\gamma=0.373$ Å^{-1}. $H^{(j)}_{\perp}$, finally, includes the π-electron hopping perpendicular to the chains.

$$H^{(j)}_{\perp}=\tfrac{1}{2}\sum_{i,j',\sigma,\sigma'}t_{i\perp}(c^{\dagger}_{j,i,\sigma}c_{j',i,\sigma}+c^{\dagger}_{j',i,\sigma}c_{j,i,\sigma}) \ . \tag{9}$$

Only the interchain hopping between nearest-neighbor sites (sites denoted by i) on adjacent chains (chains j and j') is included in this expression ($t_{i\perp}$). As pointed out by Mizes and Conwell,[14] this simplification neglects the energy dependence of the interchain hopping. However, the more distant hopping terms influence most strongly the electronic structure at the bottom and top of the π band, whereas the energy levels around the Fermi energy are essentially unaffected. Since we are mostly interested in the region around the Fermi energy, the restriction to include only nearest-neighbor interchain hopping is fully justified.

The interchain hopping is approximated to take two different values only; if site i is opposite to a positive sodium counterion [$i=i_n$, see Eq. (5)], the interchain hopping is enhanced compared to the hopping between sites not coinciding with positions of the counterions. This enhancement is due to the fact that the counterion increases the effective attractive potential of the atoms on the neighboring chain. Calculations of the interchain hopping for the tridiagonal structure in the presence of counterions show that this enhancement is about a factor 2.4.[15] The parameter used here for ordinary interchain hopping is 0.1 eV.[20] Thus, the interchain hopping between sites opposite to counterions is 0.24 eV. Note that when the doping increases, more and more counterions are intercalated between the polymer chains that cause a strengthening of the interchain hopping and therefore an *increase in the interchain interactions with increasing dopant concentration.*

It should also be noted that both $H_{\text{el-el}}$ and H_C include interchain interactions, in the first case in terms of electron-electron repulsion between charges on neighboring chains and in the second case from Coulomb attractions between the π electrons on one chain and the oppositely charged dopants associated with neighboring chains. The later effect is shown below to be of particular importance as concerns the electronic structure of the system (see Sec. III B).

The strong electron-phonon coupling in quasi-one-dimensional systems makes it necessary to perform geometry optimizations of the polymer chains for each dopant concentration. The ground-state geometry can be derived using a self-consistent iterative method developed earlier.[21] The total energy of the system described by the Hamiltonian given in Eqs. (1)–(9) is

$$E=\sum_{i,\sigma,j}[-2(t_0-\alpha v_{j,i,i+1})P^{\sigma}_{j,i,i+1}+V^{\text{imp}}_i P^{\sigma}_{j,i,i}]+\frac{K}{2}\sum_{i,j}v^2_{j,i,i+1}$$
$$+\tfrac{1}{2}\sum_{i,i'}\sum_{\sigma,\sigma'}\sum_{j,j'}U_{i,i'}(P^{\sigma'}_{j',i',i'}P^{\sigma}_{j,i,i}-P^{\sigma'}_{j',i',i'}P^{\sigma}_{j,i,i}\delta_{i,i'}\delta_{\sigma,\sigma'}\delta_{j,j'})+\sum_{i}\sum_{\sigma}\sum_{j,j'}t_{i\perp}P^{\sigma}_{j,j',i,i} \ , \tag{10}$$

where $P^{\sigma}_{j,i,i}$, $P^{\sigma}_{j,i,i+1}$ and $P^{\sigma}_{j,j',i,i}$ are elements of the density matrix obtained from the solution of the Schrödinger equation. (Density matrix elements indexed with both j and j' denote the bond order between sites on different chains.)

Minimization of the total energy with respect to $v_{j,i}$ gives the condition[21]

$$v_{k,i,i+1}=\frac{\alpha^2}{K}\left[\frac{CK}{\alpha}+2\sum_{\sigma}P^{\sigma}_{j,i,i+1}+Z\right] \ . \tag{11}$$

Z contains derivatives of the density matrix with respect to $v_{j,i}$. Since these derivatives cannot be evaluated analytically, it is convenient to neglect them during the iteration process. The final self-consistent solution is the same whether Z is neglected or not, because when self-consistency is reached, we have $Z=0$ for the system at equilibrium.

The density of states per site, $N(\varepsilon)$, is calculated from

$$N(\varepsilon)=-\frac{2}{\pi}\,\text{Im}\,\text{Tr}G(\varepsilon) \ , \tag{12}$$

where $G(\varepsilon)$ is the resolvent operator of the Hamiltonian given in Eq. (1), i.e., $G(\varepsilon)=(\varepsilon-H)^{-1}$. In order to avoid divergences in the density of states, we make the substitution $\varepsilon\rightarrow\varepsilon+i\tau$. This substitution introduces a Lorentzian-shaped broadening of the eigenenergies and gives rise to a nonzero density of states in the energy gap. The value of τ is set to 0.03 eV.

As stated above, the calculations are performed on a

system consisting of three chains. This system, including the potential from the counterions, form approximately an isolated column in sodium-doped *trans*-$(CH)_x$, which makes it a good model system for the real material.[17] In our calculations, the chain length is $N=120$, 126, or 128 carbon atoms depending on the dopant concentration, i.e., a total of 360–384 carbon atoms are included in the system. The geometry is optimized and the electronic structure calculated for dopant concentrations: $y=0.047$ ($N=126$), $y=0.067$ ($N=120$), $y=0.083$ ($N=120$), $y=0.10$ ($N=120$), $y=0.111$ ($N=126$), and $y=0.125$ ($N=128$).

In the first set of calculations, the counterion distribution is perfectly regular. We have also studied the effects of disorder on the geometrical and electronic structure of the system described above. Disorder effects are well known to produce tails in the energy bands of regular systems, and in such a way reduce the energy gap between the valence and the conduction bands. In order to study the importance of such an effect, we let the counter ions be randomly displaced from their regular positions. The distribution of the displacement is rectangular with a maximum displacement of 25% of a carbon-carbon distance. The average counter-ion separation is the same as in the regular case and that the maximum change in the counter ion separation, compared to the regular case, is half of a C-C bond (projected onto the chain axis). A stronger disorder is not expected since that would lead to a substantial increase in the Coulomb repulsion energy between the counterions. Furthermore, x-ray-diffraction studies of Rb-doped poly(phenylene-vinylene) show that the rms displacement of the dopant ions is ~ 0.4 Å at room temperature,[22] which is similar to the value used in this study. Note that, in our model, the interchain hopping is not affected for this type of disorder; the disorder appears therefore only in the diagonal of the Hamiltonian matrix.

The geometry is optimized for ten different random generations of the counter-ion positions at dopant concentrations $y=0.067$, and 0.111. The energy gap and the density of states at the Fermi energy for these systems are compared with those of the random system.

III. RESULTS

A. Lattice conformation

The optimized dimerization order parameter for each of the three chains in the system described above is shown in Fig. 2 together with the net atomic charges for one of the chains. The dopant concentrations is $y=0.10$, corresponding to a soliton-antisoliton distance of 10 CH units. The order parameter describes a perfectly regular soliton lattice. Since the spacing between two adjacent solitons corresponds to an even number of sites, there are two types of solitons along the polymer chain.[23] This is seen very clearly in the net atomic charges, which exhibit a sharp maximum at the center of the "type-1" soliton and a more extended distribution corresponding to a "type-2" soliton.

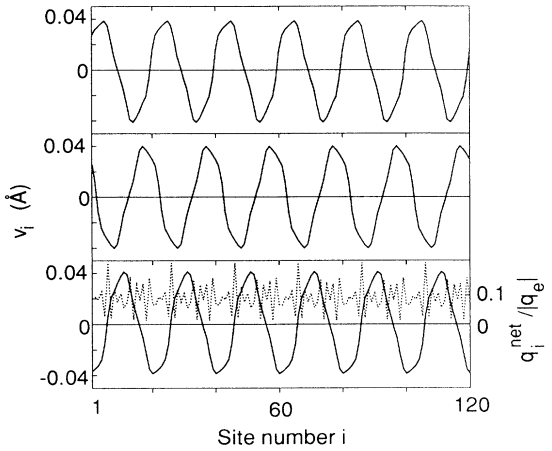

FIG. 2. Optimized dimerization order parameter and net atomic charges (dotted line) at dopant concentration $y=0.10$.

The most important effect of the interchain interaction is to produce an ordering of the phase of the dimerization order parameter between the chains. In the ground state, the ordering is such that the in-phase alignment of the dimerization order parameter on neighboring chains is minimized (see Fig. 2). The energy increase per carbon site in the case of an in-phase alignment between two adjacent chains is $\Delta E=t_\perp^2/\pi t_0$.[3] Since the system contains three chains, it is not possible to avoid the in-phase ordering completely; approximately $\frac{1}{3}$ of the system is forced to have the unfavorable interchain ordering. Note, however, that the dimerized lattice is stabilized due to the interchain interactions since a major part of the chains are aligned out of phase with respect to each other.

The external potential, i.e., the attractive dopant potential and the repulsive electrostatic potential due to the electrons on neighboring chains, is observed to affect the charge distribution and, via the electron-phonon coupling, the geometry of the chains. The effect is more pronounced when the dopant concentration is low, since in this case, the individual minima in the potential do not overlap to the same extent as in heavily doped systems. The external potential is plotted in Fig. 3 (bottom) together with the net atomic charges and the dimerization order parameter for a single chain ($y=0.067$). A charge accumulation is observed to occur around each local minimum in the external potential. This additional charge induces two weak polaronlike defects between each soliton antisoliton pair. The effect of these defects on the electronic structure is discussed in Sec. III B below.

In order to test the stability of the soliton lattice versus the polaron lattice and an undimerized lattice, we have studied the electronic structure using the following trial function for u_i ($v_{i,i+1}=u_{i+1}-u_i$):[2]

$$u_i=(-1)^{i+1}u_0\prod_n^{N_P}\left\{1+\frac{1}{\sqrt{2}}\left[\tanh\left[\frac{i-i_n-M}{l_P}\right]-\tanh\left[\frac{i-i_n+M}{l_P}\right]\right]\right\}. \quad (13)$$

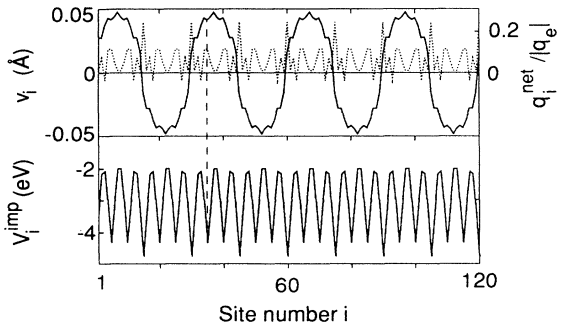

FIG. 3. Optimized dimerization order parameter, atomic charges (dotted line), and interchain electrostatic potential (bottom), at dopant concentration $y=0.067$.

The parameters u_0, M, and l_P are varied in order to obtain the minimum energy configuration. The results show that when the dopant concentration is increased, the dimerization amplitude (u_0) reduces and the geometrical defect associated with the polaron becomes less accentuated. At a dopant concentration of $y=0.067$, the polaron lattice is observed to be unstable relative to the undimerized lattice ($u_0=0$). This result is in qualitative agreement with earlier observations.[10,11] However, these authors did not include the counterion potential in their calculation, which resulted in a transition into an undimerized lattice at very low dopant concentrations. Our results show that the counterion potential stabilizes the polaron lattice relative to the undimerized lattice up to a critical dopant concentration where the minima in the dopant potential become too weak to be able to localize enough charge to create a polaron.

The results of using the trial function in Eq. (13) instead of the optimized dimerization order parameter show very clearly that neither the polaron lattice nor the undimerized lattice are stable in heavily doped *trans*-$(CH)_x$; the stable configuration corresponds instead to a soliton lattice (see above). The total energy per site of the undimerized lattice lies 5.4 meV above that of the soliton lattice at $y=0.067$. This energy difference decreases with increasing dopant concentration since the dimerization order parameter for the soliton lattice also decreases. At $y=0.111$, where the dimerization amplitude of the soliton lattice is 0.032 Å, the energy difference is 2.5 meV per site, i.e., the soliton lattice is considerably more stable than the undimerized lattice even well into the metallic regime.

Despite the small amplitude of the dimerization order parameter for the soliton lattice, charge oscillations along the polymer chains are still present up to the highest dopant concentration included in this study (see Fig. 2). This result is consistent with the observed existence of infrared-active-vibration (IRAV) modes for all dopant concentrations up to saturation doping in $K_y(CH)_{1-y}$.[24] It should be noted that charge oscillations also exist in the case of an undimerized lattice. These oscillations are entirely due to the variations in the counterion potential, i.e., charge accumulates in the vicinity of these ions, and are considerably smaller than in the case of a soliton lattice. A transition from a soliton lattice to an undimerized lattice should therefore give rise to a shift or intensity change of the IRAV modes. Since such phenomenon has not been observed, there is no support for the undimerized lattice model to explain the metallic state of heavily doped *trans*-$(CH)_x$.

B. Energy gap and density of states at the Fermi energy

The energy gap E_g and the density of states at the Fermi energy $N(\varepsilon_F)$ at various dopant concentrations are displayed in Fig. 4. The energy gap is 0.22–0.25 eV in the regime $y=0.047$–0.083. At higher dopant concentrations, there is an abrupt decrease in the energy gap to a value around 0.1 eV. At the highest dopant concentration included in this study $y=0.125$ the gap is essentially closed, i.e., the difference in energy between the levels around the Fermi energy is close to the average separation between the levels in the π band. Experimental estimates of the electronic gap have been made from optical-absorption measurements.[8] These data indicate an energy gap of around 0.2 eV at $y=0.067$, in very close agreement with our calculated single-particle gap.

The calculated density of states at the Fermi energy exhibits a sharp increase around $y=0.09$ as a result of the decrease in E_g around this dopant concentration. A maximum value of 0.102 states/(eV and carbon atom) is obtained for $y=0.125$. In fact, this value is close to the saturation value for the density of states in the middle part of the π band, since the energy gap around the Fermi energy is of the same magnitude as the average energy separation between the states within the π band. The calculated behavior of $N(\varepsilon_F)$ is in qualitative agreement with the experimental observation of a sharp increase in χ_P [$\chi_p \propto N(\varepsilon_F)$] at $y=0.06$ followed by a saturation at higher dopant concentrations. The experimentally deduced density of states in the metallic regime is 0.1 states/eV in perfect agreement with our calculated value. We can therefore conclude that the soliton lattice produces an electronic structure which is in good overall agreement with experimental data. This result, together with the result of the geometry optimizations, strongly supports the explanation of the metallic state of heavily doped *trans*-$(CH)_x$ in terms of a soliton lattice.

In order to show the importance of interchain hopping

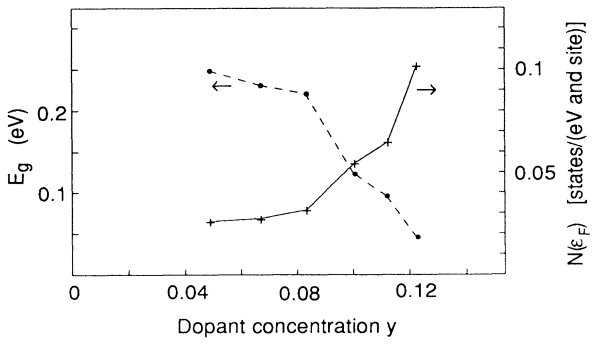

FIG. 4. Energy gap (●) and density of states at the Fermi energy (+) as a function of dopant concentration.

TABLE I. The electronic gap at different dopant concentrations (y) for zero interchain hopping ($H_\perp=0$), the counterion potential neglected ($H_C=0$), and the potential due to the counterions associated with other chains neglected ($H_C^{(j')}=0$).

	$H_\perp=0$ (eV)	$H_C=0$ (eV)	$H_C^{(j')}=0$ (eV)	Full Hamiltonian (eV)
$y=0.067$	0.4231	0.2253	0.8557	0.2334
$y=0.083$	0.4509	0.2081	0.6752	0.2233
$y=0.100$	0.3414	0.1065	0.5439	0.1222
$y=0.111$	0.3298	0.0755	0.6491	0.0988

and interchain electrostatic interactions, respectively, we have studied the influence of various terms in the Hamiltonian given in Eq. (2) on the energy gap of the system of doped *trans*-$(CH)_x$. Three different cases are considered (In all cases, the dimerization order parameter has been optimized.), case 1, $H_\perp=0$, i.e., the interchain hopping is set to zero; case 2, $H_C=0$, the counterion potential is neglected; and case 3, for each chain, the potential due to the counterions associated with other chains is neglected ($H_C^{(j')}=0$). The gap energies in the electronic spectra corresponding to the three cases are listed in Table I and compared with the result of the full Hamiltonian.

As already discussed, neglecting the interchain hopping results in an increase of the electronic gap. The effect is enhanced with increasing dopant concentration since the relative number of hopping bridges associated with the dopants is increased. Clearly, the metallic state is not obtained if the interchain hopping is set to zero, at least not for dopant concentrations below $y=0.125$. Therefore, the metallic state of heavily doped *trans*-$(CH)_x$ can only be explained within a model which includes interchain hopping.

In the case of n-type doping, the soliton levels are stabilized by the attractive potential of the counterions. Therefore, neglecting this potential causes an increase in the energy of the occupied soliton levels and a corresponding reduction of the energy gap between the soliton band and the conduction band. This effect is, however, rather small. At high dopant concentrations it is due to the fact that the minima in the dopant potential overlap strongly, which results in a nearly constant dopant potential anyway. For less heavily doped samples, e.g., at $y=0.067$, the situation is more complicated. The relatively small increase in the band gap in going from $y=0.083$ to 0.067 is due to the fact that at lower concentration there is a substantial charge accumulation in the regions opposite to counterion-soliton complexes of the neighboring chains (see Fig. 3). The geometrical distortions in these regions lead to the formation of gap states and consequently a reduction of the energy gap. This effect explains the decrease in the gap in the case of $H_\perp=0$, in going from $y=0.083$ to 0.067. The variations in the external potential at low dopant concentration thus lead to energy tails in the soliton and conduction bands and consequently to a smearing out of the energies for transitions between these bands. This effect might be as important as quantum fluctuations[25] to explain the broad absorption band of doped *trans*-$(CH)_x$.[26]

When the potential due to the counterion-soliton complexes on adjacent chains is set to zero (column three in Table I), there is a large increase in the gap. The potential minima opposite to the solitons are more pronounced in this case since the counterions in the region between the solitons are neglected. The states in the soliton band, which are localized in the vicinity of the potential minima, are therefore stabilized compared to the extended states of the conduction band. Consequently, in order to obtain a low-band-gap system it is essential that the variations in the counterion potential are small along the polymer chain. [The variations in the gap energies shown in column 3 in Table I are due to the nature of the different types of solitons. In the cases where the separation between adjacent solitons is odd, i.e., both solitons are of type 1,[23] the energy gap is enhanced. This is due to the fact that the charge associated with this type of soliton is strongly peaked at the minima in the counterion potential. The energy of the corresponding soliton states is therefore lower than in the case where type-2 solitons are present (cf. Fig. 3).]

C. Disorder

The different types of interactions included in the Hamiltonian used for these studies introduces different possibilities of disorder. Some of these possible types of disorder have already been studied. Irregularities in the intrachain hopping caused by lattice fluctuations are well known to lead to a considerable band tailing and a corresponding reduction of the energy gap.[26] Disorder in the interchain hopping is also known to introduce band tailing.[12] Both of these effects lead to a shift towards lower gap energies of the system, which results in a transition into a metallic state at lower dopant concentration than for the perfectly regular system.

Another source of disorder might come from irregularities in the positions of the counterions. As discussed above, local minima in this potential lead to charge accumulation on the polymer chain and to the creation of gap states. However, this effect is expected to be important only in the regime of low dopant concentrations, because when the concentration of counterions is high, these ions are fixed in position due to the strong repulsive interaction between adjacent ions. Furthermore, since the potential is quite smooth at high dopant concentrations, the fluctuations will also be small. For the dopant concentrations included in this study, the effect on the energy gap and density of states at the Fermi energy is very small. This result contrasts from a previous study treating the same kind of disorder, but in a strictly one-dimensional system (single chain).[23] The broadening of the band edges due to the interchain hopping hides band tailing

caused by the disorder. In the ten samples with different random counterion distributions, a maximum difference in the energy gap of about 0.03 eV was obtained, independently on the dopant concentration. Compared to the effect of $H_\perp$, which reduces the energy gap by about 0.2 eV, disorder in the positions of the counterions is clearly of minor importance.

D. Interchain delocalization

Since most calculations of the electronic structure of doped conjugated polymers are performed on single chains, there is little discussed in the literature about interchain delocalization of the electronic states. In particular, it is interesting to study the delocalization of the states closest to the energy gap, in this case, the states in the fully occupied soliton band and states at the bottom of the conduction band.

At the dopant concentrations above 5% ($y > 0.05$) the solitons on the same chain are strongly interacting. The wave functions associated with the states in the soliton band are therefore extended over the whole chain and instead of being localized to a single soliton defect, they correspond to the Bloch type of wave functions in the soliton lattice. If the interchain hopping strength ($t_\perp$) is turned on gradually we observe a delocalization of the wave functions of the soliton band over more than one chain. Figure 5 shows the state density (squared amplitude of the wave function) on each chain for one typical molecular orbital in the soliton band. The dopant concentration is $y = 0.10$. The data are plotted as a function of $\eta t_\perp$, where $\eta = 1$ corresponds to the values of the interchain hopping that are considered in the calculations presented above ($t_\perp = 0.1$ and 0.24 eV, respectively). The calculations, which include geometry optimizations, are performed on systems with fixed end boundary conditions in order to account for the finite mean free path which is always present in real systems.[27]

Figure 5 shows that there is a smooth transition from interchain delocalization to interchain localization in the regime $\eta = 1$ to 0. This is in contrast to the results derived by Firsov[28] that indicate an abrupt transition from extended to localized states at a critical interchain hopping

$$t_{\perp c} \cong \frac{0.3\hbar}{\tau} . \tag{14}$$

The reason why we observe a much smoother transition is probably due to the limitation to three chains in our system. Using the value for the scattering time τ estimated from measurement of the thermopower by Javadi *et al.*,[29] $\tau = 2.7 \times 10^{-15}$, the value of the critical interchain hopping is 0.07 eV, which is not very different from the results presented in Fig. 5.

The mean free path $l = v_F \tau$ is in our case equal to the chain length since the chains are perfectly ordered. If, however, periodic boundary conditions are used, there is no scattering of the electrons which corresponds to an infinite relaxation time τ. Three-dimensional delocalization occurs in this case for infinitesimally small values of $t_\perp$.

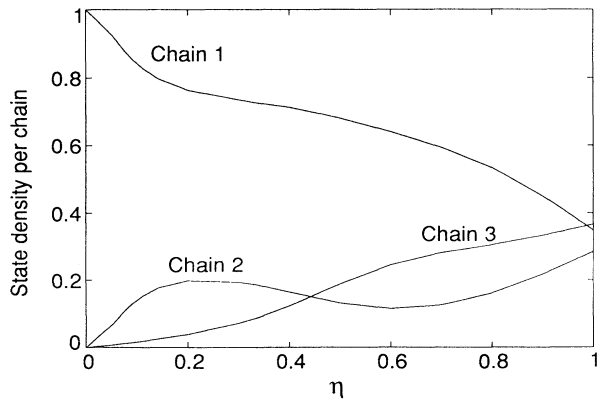

FIG. 5. State density for chains 1–3 as a function of the fraction η of the full interchain hopping.

IV. SUMMARY

The effect of interchain interactions on the electronic structure of heavily doped *trans*-$(CH)_x$ has been studied in detail for a realistic system corresponding to sodium-doped polyacetylene. A transition into a metallic state is observed around a dopant concentration of 9%. The geometrical structure of the polymer chains corresponds to a soliton lattice for all dopant concentrations we have studied. The optimized dimerization amplitude in the metallic regime is less than half of the dimerization amplitude of the pristine system. In this situation, the narrow Peierls gap can be closed by the broadening of the electronic bands due to interchain hopping.

The dopant potential is shown to play an important role in creating a metallic state. For lightly doped samples, the minima in the dopant potential in the region of the solitons stabilize the soliton states relative to the states in the conduction band. This effect increases the gap between the occupied soliton band and the conduction band, i.e., increases the gap around the Fermi energy. In the heavily doped regime, the potential is almost constant along the chain and there is no stabilization of the soliton band relative to the conduction band. Thus, the dopant potential also works in favor of a low-band-gap system when the dopant concentration is increased.

The effects of lattice fluctuations and disorder are well known to lead to band tailing and a reduction in the electronic gap. By taking such effects into account, the transition into a metallic state will occur at lower dopant concentration than for the perfect and static lattice that is treated here. It is important to note, however, that the observation of charge oscillation along the chain caused by the presence of solitons along the chain are essential in order to explain the IRAV modes that exist up to very high dopant concentrations.[24] Lattice fluctuations and disorder are therefore not expected to destroy the soliton lattice completely.

The attraction of electrons on one chain by the positive

atom cores on neighboring chains gives rise to electronic states extended over all three chains in the system. The localization of individual states as a function of the strength of this interaction (interchain hopping) is studied. At full interchain hopping, the state density on a single chain is roughly the same for all the three chains in the system. Thus, realistic values of the interchain hopping lead to three-dimensional delocalization of electrons, which in combination with the observed small gap energies is responsible for the high conductivity.

ACKNOWLEDGMENTS

The author would like to thank the Swedish Natural Science Research Council (NFR) and the Swedish Research Council for Engineering Sciences (TFR) for financial support.

[1]W. P. Su, J. R. Schrieffer, and A. J. Heeger, Phys. Rev. Lett. **42**, 1698 (1979).
[2]S. A. Brazovskii and N. Kirova, Pis'ma Zh. Eksp. Teor. Fiz. **33**, 6 (1981) [JETP Lett. **33**, 4 (1981)].
[3]D. Baeriswyl and K. Maki, Phys. Rev. B **28**, 2068 (1983).
[4]H. Naarmann and N. Thiophilou, Synth. Met. **22**, 1 (1987).
[5]J. Tsukamoto and A. Takahashi, Synth. Met. **41-43**, 7 (1991).
[6]S. Ikehata, J. Kaufer, T. Woerner, A. Pron, M. A. Druy, A. Sivak, A. J. Heeger, and A. G. MacDiarmid, Phys. Rev. Lett. **45**, 1123 (1980).
[7]J. Chen and A. J. Heeger, Synth. Met. **24**, 311 (1988).
[8]X. Q. Yang, D. B. Tanner, M. J. Rice, H. W. Gibson, A. Feldblum, and A. J. Epstein, Solid State Commun. **61**, 335 (1987).
[9]M. Novak, S. D. D. V. Rughooputh, S. Hotta, and A. J. Heeger, Macromolecules **20**, 965 (1987).
[10]P. Vogel and D. K. Campbell, Phys. Rev. Lett. **62**, 2012 (1989).
[11]D. Baeriswyl and K. Maki, Synth. Met. **28**, D507 (1989).
[12]M. Wolf and K. Fesser, J. Phys. Condens. Matter **3**, 5489 (1991).
[13]S. Stafström, in *Electronic Properties of Polymers,* edited by H. Kuzmany, M. Mehring, and S. Roth, Springer Series in Solid-State Sciences Vol. 107 (Springer-Verlag, Berlin, 1992), p. 11.
[14]H. A. Mizes and E. M. Conwell, Phys. Rev. B **43**, 9053 (1991).
[15]R. J. Cohen and A. J. Glick, Phys. Rev. B **42**, 7658 (1990).
[16]M. Winokur, Y. B. Moon, A. J. Heeger, J. Barker, D. C. Bott, and H. Shirakawa, Phys. Rev. Lett. **58**, 2329 (1987).
[17]D. Chen, M. J. Winokur, M. A. Masse, and F. E. Karasz, Phys. Rev. B **41**, 6759 (1990).
[18]E. M. Conwell, H. A. Mizes, and S. Jeyadev, Phys. Rev. B **40**, 1630 (1989).
[19]H. Fukutome and M. Sasai, Prog. Theor. Phys. **69**, 373 (1983).
[20]P. M. Grant and I. P. Batra, Solid State Commun. **29**, 225 (1979).
[21]S. Stafström and K. A. Chao, Phys. Rev. B **29**, 7010 (1984).
[22]M. J. Winokur (unpublished).
[23]S. Stafström, Phys. Rev. B **43**, 9158 (1991).
[24]D. B. Tanner, G. L. Doll, A. M. Rao, P. C. Eklund, G. A. Arbuckle, and A. G. MacDiarmid, Synth. Met. **28**, D141 (1989).
[25]A. Takahashi, Phys. Rev. B **46**, 11 550 (1992).
[26]A. Feldblum, J. H. Kaufman, S. Etemad, A. J. Heeger, T. C. Chung, and A. G. MacDiarmid, Phys. Rev. B **26**, 815 (1982).
[27]S. Kivelson and A. J. Heeger, Synth. Met. **22**, 371 (1988).
[28]Y. A. Firsov, *Localization and Metal-Insulator Transition,* edited by H. Frizsche and D. Adler (Plenum, New York, 1985).
[29]H. H. S. Javadi, A. Chakraborty, C. Li, N. Thiophilou, D. B. Swanson, A. G. MacDiarmid, and A. J. Epstein, Phys. Rev. B **43**, 21 831 (1991).